CHIN. PHYS. LETT. Vol. 31, No. 9 (2014) 094601

Crack Arrest in Brittle Ceramics Subjected to Thermal Shock and Ablation *

WANG Yan-Wei(王艳伟)[1,2], YU He-Long(于合龙)[3], TANG Hong-Xiang(唐翊翔)[1,2], FENG Xue(冯雪)[1,2**]

[1] *AML, Department of Engineering Mechanics, Tsinghua University, Beijing 100084*
[2] *Center for Mechanics and Materials, Tsinghua University, Beijing 100084*
[3] *College of Information Technology, Jilin Agricultural University, Changchun 130118*

(Received 1 May 2014)

Ceramics are suitable for high temperature applications, especially for aerospace materials. When serving in high temperature environments, ceramics usually have to deal with the challenge of both thermal shock and ablation. We report the crack arrest in brittle ceramics during thermal shock and ablation. In our experiment, the specimens of Al_2O_3 are subjected to oxygen-propane flame heating until the temperature arises up to 1046°C and then are cooled down in air. The crack occurs, however, it does not propagate when arrested by the microstructures (e.g., micro-bridges) of the crack tip. Such micro-bridge enhances the toughness of the brittle ceramics and prevents the crack propagation, which provides a hint for design of materials against the thermal shock.

PACS: 46.50.+a, 81.05.Mh DOI: 10.1088/0256-307X/31/9/094601

Ceramics are suitable for high temperature applications, such as engine parts of aerospace materials, nozzles and thermal protection systems of the space shuttle, due to their high melting points, chemical and physical stability and excellent corrosion resistance in high temperature environments.[1] When serving in high temperature environments, ceramics usually have to deal with the challenge of both thermal shock and ablation.[2–4] For instance, thermo parts in rocket engine are subjected to thermal shock first when oxygen propane is ignited, and subsequent ablation during stable burning.[5] It may imply the working temperature can be raised to enhance the overall performance if ceramics have excellent thermal shock resistance[6] and mechanical properties. In order to improve their strength, toughness, thermal shock resistance and high-temperature stability, lots of efforts have been made so far. When the thermal stress[7] exceeds the critical stress, a crack will propagate and cause brittle failure in the structure.[8–10] Winkelman and Shott first defined the property of thermal stress resistance in 1894.[11] Subsequently, many experiments and analyses were carried out to investigate the fracture of brittle materials subjected to thermal shock.[12–14] Moreover, ablation usually follows the thermal shock during applications in engine and therefore becomes the concern to assess its durability.[15] However, there are only a few studies on both thermal shock and ablation to imitate real working conditions.

In this Letter, we report our experimental investigations and then provide a fundamental understanding of the ablation and thermal shock for brittle ceramics. The microstructure features of the specimens before and after thermal shock observed by scanning electron microscopy (SEM) also provide considerable evidence to reveal the mechanism of crack arrest in the ceramics.

The square specimens used in this experiment are 96% alumina ceramics (Al_2O_3) with the thickness of 1 mm and length of 35.5 mm, which were made by the tape-casting technique. The bulk density of the materials is 3.74 g/cm^3. Grain size is 3–5 μm, elastic modulus E is 386 MPa, thermal tensile strength σ_f is 320 MPa, Poisson's ratio ν is 0.254, coefficient of thermal expansion α is 6.5 K^{-1}, thermal conductivity k is 24 W/(mK), and thermal diffusivity a is 8 W·(mK)$^{-1}$. The fracture toughness K_{IC} is 4 MPa·m$^{-1/2}$. Then we can obtain the thermal shock resistance R to be 95 K. The specified setup was designed to conduct the real-time, full-field and in-situ measurement of thermal shock and ablation. During the experiment, the output pressure of the oxygen was 0.5 MPa. The output pressure of propane was 0.09 MPa. The oxygen-propane flame was elaborately controlled and moved close to the specimen, and the infrared pyrometer and high speed camera were used to record the temperature field and morphology change of the observation surface of the specimen respectively. Then the specimens were subjected to thermal shock first and then ablation by the flame. Before the test, we drew the grid on the surface of Al_2O_3 specimens by using graphite. The graphite grid would disappear when it was heated above 400°C. Therefore, we used this property of the graphite to observe the temperature distribution and gradient by the high speed camera system.

*Supported by the National Natural Science Foundation of China under Grant Nos 11227801, 11222220, 91116006, 10902059, 11372155 and 1320101001, and the Tsinghua University Initiative Scientific Research Program under Grant No 2011Z02173.

**Corresponding author. Email: fengxue@tsinghua.edu.cn

© 2014 Chinese Physical Society and IOP Publishing Ltd

The results of the thermal shock tests show that most of the specimens would spall into pieces with temperature below 600℃.[16] Surprisingly, twenty percent of repeated specimens did not break after thermal shock even the temperature of ablation was above 1000℃. Thus we focus on these specimens and analyze the mechanism of such behavior which has a high resistance to thermal shock and ablation.

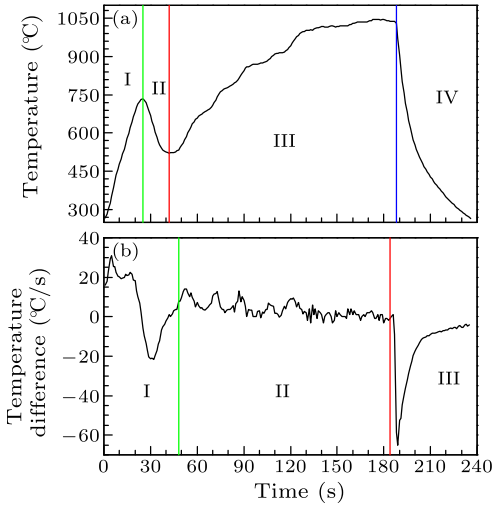

Fig. 1. Temperature of the surface specimen: (a) the heated temperature curve, (b) the rate of temperature change.

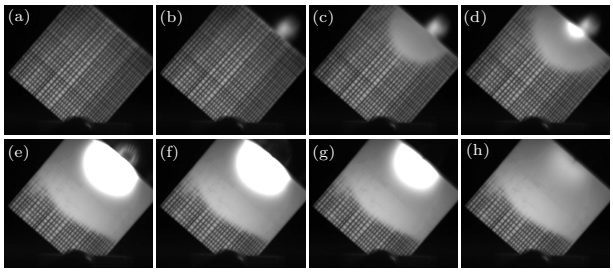

Fig. 2. Images of specimen subjected to thermal shock and ablation at different times. (a) Initial specimen when the frame was turned on; (b) $t = 1$ s, (c) $t = 26$ s, (d) $t = 87$ s, (e) $t = 175$ s, (f) $t = 188$ s, (g) $t = 189$ s and (h) $t = 192$ s after the initial reference time.

The specimen was subjected to the thermal loading as follows: thermal shock (hot shock), ablation and thermal shock (cold shock) during the experimental process. Figure 1(a) shows the temperature of the heating area of specimen versus the time. There are four zones for the temperature evolution. At the beginning (zone I), thermal shock occurred when the specimen was subjected to the flame suddenly. It is found that temperature increases quickly and is almost linear with the time. The rate curve of temperature change in Fig. 1(b) is the difference quotient of the temperature curve. Correspondingly, we can obtain the transient maximum ascendant temperature difference to be 30.9℃/s from Fig. 1(b). Usually 80% of the specimens spalled into pieces when the temperature was below 600℃. However, 20% of the specimens did not break into pieces. Then we slowed down the moving speed of the flame towards the specimen. When the speed of the flame was adjusted, the machine had to stop the flame moving, so that the temperature rapidly dropped to 521.8℃, as shown in zone Ⅱ. At the time of 43 s, zone Ⅲ began for ablation test. The temperature increased smoothly. Finally we shut down the flame, then the specimen turned to cold shock again in the ambient air, as shown in zone Ⅳ. From Fig. 1(b), we can find that, after turning off the flame, the average ascendant temperature difference is 54.5℃/s within 5 s and the maximum transient temperature difference is 65.2℃/s in this period without breaking of the specimen yet.

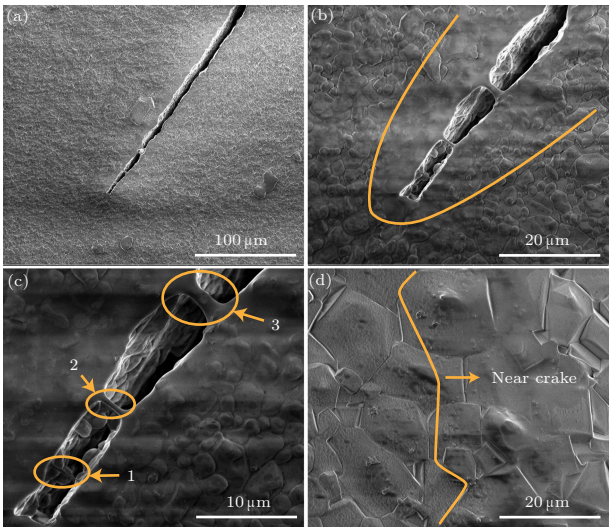

Fig. 3. SEM images of micro-crack and surface around the heated spot after the test: (a) micro-crack configuration, (b) microstructure of the micro-crack, (c) micro-bridges in micro-crack, and (d) transition zone from grains to melting area near crack.

Figure 2 shows the sequential images of specimen subjected to thermal shock and ablation captured by the high speed camera. From the disappearing of the grid, we could find the evolution of full-field temperature during heating. Figure 2(a) shows that the specimen with grids before the fire was turned on ($t = 0$). Figure 2(b) shows that the oxygen-propane flame was fired on and kept off from the specimen for a short while till the flame became stable. Figure 2(c) shows that the flame was moved to the mid-point of the edge of the specimen ($t = 26$ s), specimen reached the first maximum temperature 733.6℃ and the specimen was subjected to thermal (hot) shock firstly, corresponding to zone I in Fig. 1(a). The specimen was subjected to ablation and still kept unbroken even with the temperature of 806.2℃, as shown in Fig. 2(d). The temperature distribution and its gradient can be inferred by three different areas in the image: the light area

for high temperature, the middle area without grid above 400℃ and the area with grid below 400℃. Figure 2(e) shows the image of specimen when the maximum temperature of the specimen was 1046℃. Figure 2(f) shows the image when the flame was shut off. Then the specimen was subjected to cold shock in the ambient air after 1 s and 3 s shown in Figs. 2(g) and 2(h) respectively. The images clearly show that the specimen did not break during the cold shock. However, we can find the short crack with the length of 5 mm at the heating spot when the specimen was totally cooled down to room temperature, as shown in Fig. 2(h). Usually, the brittle ceramics are very sensitive to crack and able to spall into pieces when subjected to thermal (or cold) shock.

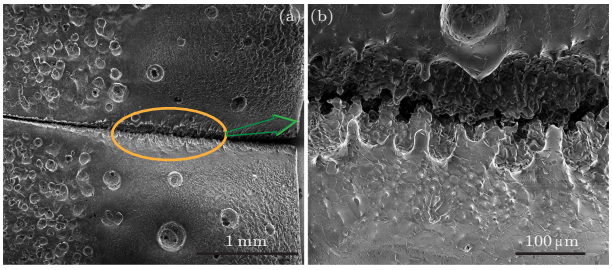

Fig. 4. SEM images of the specimen surface after ablation and thermal shock: (a) the ablation zone with the crack; and (b) zoomed micro-structure of the ablation zone.

To investigate the mechanism of such an unusual phenomenon, the microstructural features around the crack of the specimen after test were observed from the backside by scanning electron microscopy (SEM), as shown in Fig. 3. Figure 3(a) shows the morphography and configuration of the crack. Figures 3(b) and 3(c) show that there are three micro-bridges (numbered by 1, 2 and 3) in the crack tip. It is found that the width of the micro-bridges increases with the distance from the tip. Obviously, the tensile stress in the micro-bridges suppresses the mode I crack propagation. Actually, there is a transition zone from crack to normal grains, as shown in Fig. 3(d). When the crack propagates from the zone, the tensile stresses stretch the melting grain and then result into the micro-bridges structures, which enhance the toughness and thermal shock resistance of the specimen. Microstructure of the specimen surface after ablation is shown in Fig. 4. Obviously, the crack was induced by thermal shock, and then the specimen was subjected to ablation due to the fact that the surface has many tiny ablation pits. During thermal shock, the micro-bridges suppressed the crack propagation. When we zoom into the middle of the crack, we can find many broken crack bridges between the crack surfaces, as shown in Fig. 4(b). These images clearly denote the specimen survives from the thermal shock and the ablation.

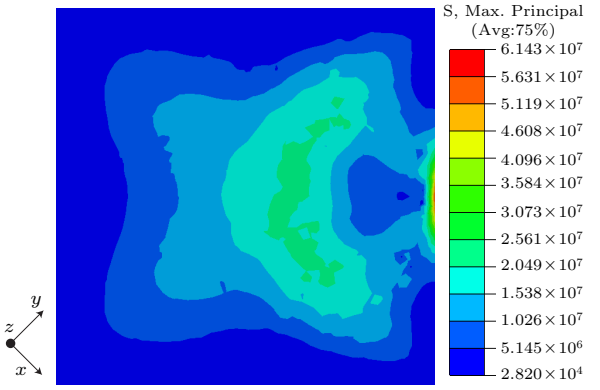

Fig. 5. The max principle stress field of Al_2O_3 ceramic.

To investigate the mechanism of such a phenomenon, the finite element method (FEM) was used to study the temperature and stress distribution during heating. Some assumptions are proposed in the numerical simulation. First, the ceramics are assumed to be isotropic, homogeneous and perfect, which means that the specimen had no flaws. Secondly, all physical properties do not relate to temperature. Thirdly, the temperature of the specimen was in accordance with the temperature of the environment. The specimen was axial symmetry, thus our simulation model was axial symmetry. The size of the specimen was 35 mm×35 mm×1 mm. The model of specimen was meshed with rectangular elements (C3D8T). The corner of specimen was fixed by a clamp. The displacements of the corner nodes were limited. The other edges were free. The hot zone was a half-circle. The radius of the hot zone was 2 mm, the center of the circle was located at the middle point of the edge of the specimen. The environment temperature was 298 K. When the temperature began to descend, the specimen was subjected to cold shock. The max principle stress reached its maximum in Fig. 5. When the specimen was subjected to the hot shock and ablation, the hot zone of the specimen was under compressive stress condition. However, when the specimen was subjected to cold shock, the hot zone was under tensile stress condition, the maximum tensile stress was at the middle of the hot zone, where the crack initiated. The stress changed severely at the beginning of cold shock. The maximum temperature gradient occurred at the symmetry axis direction of the hot zone. Correspondingly, the maximum stress gradient occurred at the same direction. When the time elapsed, the maximum temperature gradient moved along the symmetry axis of the specimen as well as the maximum stress. The location of the maximum stress moved along the symmetry axis. Therefore, the temperature gradient resulted into the nonuniform stress. The crack initiated from tensile stress, and obviously the crack propagated along the maximum

temperature gradient. The strength of the materials descended with the temperature increment. We simulated the temperature of the observation surface. The temperature of the hot zone is higher than that of the observation surface.

In the experiment process, when the crack is initiated and it propagates, the material at the heating surface might be in its liquid state, and the micro-bridge will be formed when the specimen is cooled down. The micro-bridges enhanced the crack propagation resistance.

Usually, the criteria of thermal shock resistance is the maximum temperature difference that brittle materials can be subjected to without cracking. Thus the maximum stress can be represented as

$$\sigma_{\max} = \frac{\phi\alpha E\Delta T}{1-\upsilon}, \tag{1}$$

where E is the elastic module, ΔT is the temperature difference, υ is Poisson's ratio, α is the thermal expansion coefficient, and ϕ is the stress reduction factor[17] in the range [0,1]. We also calculated the first and the second thermal shock resistance R and R' with the following equation

$$R' = kR = \frac{k\sigma_{\rm f}(1-\upsilon)}{\alpha E}, \tag{2}$$

where E is the elastic modulus, $\sigma_{\rm f}$ is thermal tensile strength, υ is Poisson's ratio, α is coefficient of thermal expansion, k is thermal conductivity, and ΔT is related to the stress reduction factor and can be represented as

$$\Delta T = \frac{R}{\phi} = \frac{R'}{\phi k}, \tag{3}$$

which indicates that the temperature difference increases as ϕ decreases with the other factors keeping the same. From Eq. (3), we can see that the thermal shock resistance is improved with decreasing ϕ. It is obvious that the micro-bridges in the crack absorb the local deformation during thermal shock. Therefore, the stress reduction factor decreases. Thus micro-bridges enhanced the thermal shock resistance and arrested the crack propagation, which suggests that we could improve the thermal shock resistance by controlling the stress reduction factor. Hence, we can find the new structure or method to improve thermal shock resistance and ablation of the alumina ceramic specimen at high temperature.

In summary, this thermal shock experiment imitates ceramic material under the real working thermal shock conditions. It is found that the micro-bridges are formed in the cooling process, which helps to increase the crack arrest of brittle specimens subjected to thermal shock. FEM is used to simulate the temperature field and stress field in the thermal shock, the results are qualitatively consistent with the experiment. This discovery can provide a novel method to improve the thermal shock resistance of ceramic materials by changing microstructure design.

References

[1] Munz D, Fett T 1999 *Ceramics: Mechanical Properties, Failure Behavior, Materials Selection* (Berlin: Springer Verlag)
[2] Lu A J 2013 *Acta Phys. Sin.* **62** 217101 (in Chinese)
[3] Wang W T et al 2013 *Acta Phys. Sin.* **62** 210601 (in Chinese)
[4] Zhang Y D et al 2013 *Chin. Phys.* B **22** 084102
[5] Xu X et al 2006 *Pure Appl. Geophys.* **163** 1751
[6] Lanin A, Fedik I 2008 *Thermal Stress Resistance of Materials* (New York: Springer)
[7] Krommer M 2004 *Acta Mech.* **171** 59
[8] Manson S S and Smith R W 1955 *J. Am. Ceram. Soc.* **38** 18
[9] Yongle S et al 2011 *Key Eng. Mater.* **462** 383
[10] Shaohua C and Tzuchiang W 2001 *Acta Mech. Sin.* **17** 269
[11] Winkelmann A and Schott O 1894 *Ann. Phys.* (Berlin) **287** 730
[12] Kingery W 1959 *Properties Measurement at High Temperature* (New York: Wiley)
[13] Pisarenko G S 1969 *High-Temperature Strength of Materials* (Washington DC: Israel Program for Scientific Translations)
[14] Hasselman D 1963 *J. Am. Ceram. Soc.* **46** 535
[15] Tang S et al 2007 *Mater. Sci. Eng.* A **465** 1
[16] Hasselman D P H 1963 *J. Am. Ceram. Soc.* **46** 229
[17] Li W G et al 2012 *Appl. Math. Mech.* **33** 1351